STATUS OF ISABELLE LATTICE*

J. Claus, M. Cornacchia, E.D. Courant and G. Parzen†

Introduction

ISABELLE, a facility for colliding protons with center of mass energies between 60 and 800 GeV, is presently under construction at Brookhaven National Laboratory. The device consists of two identical rings for the accumulation, acceleration and storage of proton beams, shaped and interlaced in the horizontal plane to intersect in six so-called crossing points where the beams that rotate in opposite directions in the two rings are exposed to each other. The overall dimensions of the facility are kept relatively small because advantage is taken of the large fields and gradients that are possible in superconducting magnets; the associated saturation effects in the magnet iron make a separated function lattice practically inevitable. The rings are to be filled from the AGS, using synchronous beam transfer; this forces their circumference to an integer multiple of the rf wavelength in the AGS ($\approx$67.26 m). The integer chosen is 57, about the lowest value possible, thus the circumference of each ring is 3833.85 m. The charge in each ring is expected to be about 6.4×10^{14} protons, which requires about 250 AGS charges of 2.75×10^{12} protons per pulse if the injection efficiency is 100%. The actual efficiency is unlikely to be better than 50%, so that in excess of 500 AGS pulses may be needed per ring. The beam is to be accumulated in synchrotron phase space by means of an injection and stacking procedure similar to one developed for the ISR at CERN; this leaves the betatron emittance of the circulating beams independent of its intensity and equal to that in the AGS just before extraction while its momentum spread increases with intensity.

The topology of the system is indicated in Fig. 1; we distinguish inner and outer arcs and inner and outer half insertions, the insertions link alternating inner and outer arcs together in two closed rings. Each ring has a basic 3-fold superperiodicity with mirror symmetric superperiods, provided that the insertions are identical among each other; the superperiodicity is very nearly 6-fold, however, again with very nearly mirror symmetric superperiods, because inner and outer arcs are very nearly identical and insertions very nearly mirror symmetric. Pairs of inner and outer arcs have common centers and a common cell structure with identical magnets. They differ only in average radius of curvature; this is necessary to make the geometry possible. One consequence is that there must be some bending in the insertions. This bending is done near the interfaces with the arcs in such a fashion that the central region of the insertions is free of dispersion. One shows easily that the angle between the two intersecting beams, the crossing angle, is equal to twice the difference in deflections in outer and inner path between successive crossing points, thus equal to the difference in the deflections in outer and inner half insertions.

Arcs

The arcs are constructed with identical magnet components (dipoles and quadrupoles), the mean radius of curvature for the inner arcs is 339.031 m, that for the outer arcs is 339.878 m, the radius of curvature in all dipoles is 266.638 m. The relative difference of 2.7×10^{-3} between inner and outer arc radius is obtained by making the drift spaces between magnet units in the outer arcs slightly longer than in the inner arcs. The excitations of focussing and defocussing quads of an arc may differ by a few percent as may the mean quad excitations of different arcs. Thus it is possible to set the horizontal and vertical betatron tunes independently of each other and to make the betatron phase advances across the outer arcs identical to those across the inner ones despite the differences in drift space-length.

---

*Work performed under the auspices of the U.S. Department of Energy.

†Brookhaven National Laboratory, Upton, NY 11973

Each arc contains 9 mirror symmetric regular cells of FoBdBdBoBDDoBdBdBoF structure (where F and D represent focussing and defocussing half quads, B a dipole, o the drift space between a quad and a dipole and d that between full dipoles). The effective length of the quads (full length) is 1.643 m, that of the dipoles 4.605 m, the dipoles generate a radius of orbit curvature $\rho = 266.638$ m, thus deflect by $\theta = 17.27$ mrad $= 0.9893°$ per unit for a total of $53.42°$ per arc. The arcs terminate on the midplanes of horizontally focussing quads, necessary for the insertion design.

Phase Advance per Cell and Number of Cells

The betatron phase advances per cell $\Delta\psi_H$ and $\Delta\psi_V$ were chosen to be about $\pi/2$ rad, corresponding with wave numbers $\psi_H \approx \psi_V \approx 22.6$ for a ring with 6 superperiods of 9 regular cells and one insertion with phase advances of 3π rad each. This choice reflects a compromise between the conflicting requirements of final energy, intensity and injection. Since we intend to accumulate beams in synchrotron phase space a maximum dispersion X_p [$= \Delta x/(\Delta p/p)$] of low value is desirable, as is a low value of the betatron amplitude function β; it is also necessary to keep the transition energy γ_{tr} sufficiently far below the injection energy γ in order to keep the phase slip factor $\eta(=1/\gamma_{tr}^2 - 1/\gamma^2)$ at a reasonable value. η and the revolution period T set the time scale for the longitudinal motion, thus for the injection and stacking operations. That scale is rather long for the present choice of $\gamma_{tr} \approx 18.68$, $\gamma = 31.4$, T = 12.8 per sec, thus $\eta = 0.00185$; it takes a particle 14 seconds ($\approx 1.1 \times 10^6$ revolutions) to gain or loose a turn on another one with an energy difference of 4.9×10^{-4}, about the total energy spread in the injected beam near the end of the stacking cycle. Another consideration is that the threshold for coherent longitudinal instabilities is directly proportional to η for fixed shunt impedance.

In a ring constructed with quadrupoles with the highest practical gradient, dipoles with the highest practical field and negligible drift space between magnetic elements the average bending field as a fraction of the actual dipole field is equal to the fraction of the ring circumference that is occupied by the dipoles. The higher that fraction, the higher the final particle energy, the less space there is for quadrupoles. After choice of that fraction there is still freedom in the distribution of the quads, i.e., in the number of cells and in the ratio between the length of horizontally focussing and defocussing quads. We consider the dependence of various parameters on the number of cells for a fixed ratio between average and actual bending fields for equal betatron tunes in the horizontal and vertical directions. We approximated the true ring structure with equally spaced point quadrupoles of equal absolute strength and equal point dipoles midway between the quads and found the following expressions for $\Delta\psi$, β, X_p and the momentum compaction α[$= (d\ell/\ell)/(dp/p)$]:

$$\sin(\Delta\psi/2) = |q\ell| \tag{1}$$

$$\beta = \frac{\ell}{\sin(\Delta\psi/2)} \sqrt{\frac{1 \pm \sin(\Delta\psi/2)}{1 \mp \sin(\Delta\psi/2)}} \tag{2}$$

$$X_p = \frac{\ell}{\sin^2(\Delta\psi/2)} [1 \pm \tfrac{1}{2} \sin(\Delta x/2)]\,\theta \tag{3}$$

$$\alpha = [1 - \tfrac{1}{2}\sin(\Delta\psi/2)^2] \cdot [\theta/\sin(\Delta\psi/2)]^2 \tag{4}$$

The expressions for β and X_p are valid in the midplanes of the quadrupoles, the raised signs applying to focussing quads, the lower ones to focussing quads. 2ℓ represents the cell length, $\pm 2q$ the inverse focal length of a quad, and 2θ the beam deflection per cell. Both q and θ are proportional to the cell length, so $q\ell =$

$(dq/d\ell)\ell^2$ and $\theta = (d\theta/d\ell)\ell$. In addition, we consider the length of the insertions fixed at a fraction λ of the superperiod length $C/6$, with C the total circumference; their phase advances are fixed at 3π rad and their momentum compaction $\alpha = 0$ because there is essentially no bending in them. With these approximations one obtains for the betatron wave numbers

$$\nu \approx \frac{6}{2\pi} \left(3\pi + \frac{1-\lambda}{2\ell} \frac{C}{6} \Delta x \right) \tag{5}$$

and for the transition energy

$$\gamma_{tr} = \left[\alpha(1-\lambda) \right]^{-\frac{1}{2}} \tag{6}$$

For the maximum beam width in the arcs one has normally

$$\hat{w} = \hat{X}_p \frac{\Delta p}{p} + 2\sqrt{\epsilon \hat{\beta}} \tag{7}$$

where ϵ is the betatron emittance of the beam and $\Delta p/p$ its (total) momentum spread. There are two separate beams of equal emittance in the ring during the injection stacking cycle so then

$$\hat{w} = X_p \left(\frac{\Delta p}{p} \right)_i + 4\sqrt{\epsilon \hat{\beta}} \tag{8}$$

If the beam current I is limited by the onset of longitudinal instabilities one has

$$I < I(\Delta p/p)^2 \eta \tag{9}$$

with I the appropriate constant, that current is maximized by minimizing ϵ and maximizing η/X_p^2 since then

$$I < I(\hat{w} - 4\sqrt{\epsilon \hat{\beta}})^2 \, \eta/X_p^2 \tag{10}$$

In Fig. 2 we plot β/β_r, X_p/X_{pr}, γ_{tr}/γ_{trr}, ν, $\Delta p/p$, $(\Delta p/p)_i$, and $(\eta/\eta_r)(X_{pr}/X_p)^2$ as functions of the cell length $\mu = \ell/\ell_r$ with $\beta_r \approx 67$ m, $X_{pr} \approx 2.75$ m, $\gamma_{tr} \approx 18.75$, $\Delta\psi_r \approx 0.2515 \times 2\pi$ and $\ell_r \approx 19.75$ m, the parameters of the presently selected lattice. The available horizontal aperture $\hat{w}$ is taken as 66 mm for an ID of the vacuum pipe of 88 mm and the (non-normalized) emittance ϵ is at injection $0.5 \times 10^{-6}\pi$ rad-m. Only values of μ given by $\mu = 9/M$ with M integer have physical significance because the number of cells per arc M must be integer. It is evident from the graphs that the chosen lattice is close to optimum under the accepted constraints of $\rho/\rho_{av} \approx 266.64/339.45 = 0.785$ and $\lambda \approx 0.444$ if the momentum acceptance $(\Delta p/p)_i = 1.57 \times 10^{-2}$ is to be maximized. If the longitudinal stability is the critical parameter it might seem advantageous to increase M from 9 to 11 since this would increase η/X_p^2 and the beam current by some 5%. The largest gain would be in the increase in η by a factor of two from 0.0018 to 0.0035, primarily because of the associated reduction in the time scale for the longitudinal motion by the same factor. The change would entrain an increase in the number of magnet units per arc from $9 \times (2+6) = 72$ to 88, however, and a reduction in the drift space lengths between the magnets by $1 - 72/88 = 0.18$, probably too much to be acceptable and one concludes that the benefit does not balance the extra effort.

Split Betatron Tunes

We considered splitting the betatron tunes by a large amount, i.e., $\nu_H = 22.6$ and $\nu_V = 19.6$ or 16.6. Among the advantages would be a reduction in the average quadrupole strength, a possibly more desirable working region in the tune diagram, a 10% reduction in β_H and a 10% reduction in $\hat{X}_p$. β is considerably larger however which is very undesirable in view of the proposed methods of injection and extraction in the vertical plane. The work was discontinued for that reason.

Insertions

The insertions determine the characteristics of the beam in the crossing points, the space available for experimental apparatus about that point and represent a major factor in the ring geometry. The crossing angle

and the overall length are crucial for the distances between inner and outer arcs; these should be held as small as possible in order to keep the tunnel cross section small. Other considerations are that changes in the betatron tune (obtained by adjustment of the phase advances in the regular arcs) should not require readjustment of the insertions and that changes in any particular insertion should not force readjustments in any of the others or in the regular arcs. The design that evolved has an overall insertion length of 283.50 m, and a crossing angle of 11.188 mrad. It imposes a distance between the center lines of homologous quadrupoles in inner and outer arcs of about 0.95 m. Fig. 3 shows the elements of an inner and an outer half insertion in proper relative position. Each half insertion consists of an 80 m long drift space, interruped by a quadrupole doublet in the middle, followed by three half cells similar to the ones in the flanking arc. These half cells contain dipoles, arranged to make the long drift space free of dispersion. The long drift space is available for experimental equipment, including quadrupoles and dipoles for control of the beam characteristics in the crossing point, the latter always under the condition that the transfer characteristics of the insertion as a whole are not change . The doublet mentioned represents the more extensively studied arrangement so far. The quadrupoles of adjacent doublets in inner and outer half insertions are staggered longitudinally to gain sufficient radial space to preserve them as physically separate and independent units. Such staggering can be done in 8 different ways. The one that is preferred at the moment has the doublets in all outer half insertions closer to the crossing points than in the inner ones. This gives the whole complex 6-fold symmetry though the superperiodicity of each ring is only 3-fold. Another has all the doublets in one ring closer to the crossing points than in the other. This gives each ring very nearly true 6-fold superperiodicity, but causes slight differences between rings. A brief study did not disclose any striking advantages so far, proof that the departure from 6-fold superperiodicity in the preferred case is rather minor.

Betatron Phase Advances

The insertions are decoupled from the betatron tunes and each other by demanding that the phase advances per cell be equal in inner and outer arcs and by giving their transfer matrices the form

$$(M) = \begin{pmatrix} m & o \\ o & 1/m \end{pmatrix} \tag{11}$$

in both reference planes with $m^2 = \ell_d/\ell_u$, the ratio of the half cell lengths in (d)ownstream and (u)pstream arcs. This is so because $\alpha = 0$ and β proportional to the half cell lengths in the interfaces with the arcs. m may be either positive or negative, corresponding with phase advances across the insertion of $2k\pi$ or $(2k-1)\pi$. Such matrices may be realized with half insertions with matrices of the form

$$\begin{pmatrix} o & a \\ -1/a & o \end{pmatrix} \text{ or } \begin{pmatrix} a & o \\ o & 1/a \end{pmatrix} \tag{12}$$

representing phase advances of $(2k-1)\pi/2$ or $k\pi$, which yield $m = \mp a_d/a_u$ respectively. The value for β^* follows from the value of β in the upstream interface via

$$\beta\beta^* = a_u^2 \text{ resp } \beta^*/\beta = a_u^2 \quad ; \tag{13}$$

evidently $|d\beta^*/\beta^*| = |d\beta/\beta|$ in both cases. It follows that the betatron match from arc to arc is preserved and that the β^*'s change only in a minor way if the betatron tunes are adjusted via equal changes in the phase advances in the arcs, thus by equal relative changes in their quad excitations, and also that changes in the relation between the β^*'s and the β's

in the interfaces do not affect that match if a_d/a_u is preserved.

The picture deteriorates when momentum dependence is taken into account. The dispersion is matched only to first order in $\Delta p/p$ in the interfaces and that only for one state of betatron tune. The dispersions of arcs and insertions depend non-linearly upon the momentum deviation in different ways so that an error develops as a function of it. The betatron phase advances across the insertions are also functions of the momentum deviation because the inverse focal lengths of the quads are so. The change in dispersion of the arcs with the phase advance per cell, thus with the betatron tune, cannot now be fully matched by adjustment of the insertion. Together these errors cause a forced oscillation of the closed orbit whose amplitude increases from zero with increasing momentum deviation.

Table I

Δ_ν	-1	-0.5	0	0.5	1
β_{xmax}(cells)	65.50	66.25	66.72	67.68	69.13
$\hat{X}_p$(cells)	3.04	2.87	2.73	2.60	2.48
β_y^*	7.5	7.01	7.5	8.05	8.63
β_x^*	40.88	41.69	41.25	40.66	39.98
X_p	-0.079	-0.075	0	0.209	0.96
X_{pmax}	3.31	3.00	2.74	2.86	3.71

Table I shows the dependence of some lattice functions on the betatron tunes for the present design which has phase advances of 3π rad per insertion. It shows the degree of mismatch and the behavior of β^* and X_p^* in the crossing point for tune changes $-1 < \Delta\nu < +1$ with respect to the nominal tune of 22.6, obtained by changing the phase shifts in the regular cells but leaving the insertions undisturbed. The mismatch present causes X_p to oscillate and to achieve large values in some of the horizontally focussing quadrupoles. Its largest value X_{pmax} is given in Table I. The extent to which this value exceeds X_p, the value of X_p in the horizontally focussing quads in a ring with ideal, i.e., perfectly matched, insertions, indicates the loss in aperture due to the mismatch. It appears possible to change ν_x and ν_y by $\Delta\nu = -1$ to $\Delta\nu = 0.5$ without being required to rematch the insertions. The phase advances across the insertions could be increased from 3π rad to 4π rad by incorporating into them one cell of the regular arcs on either side.
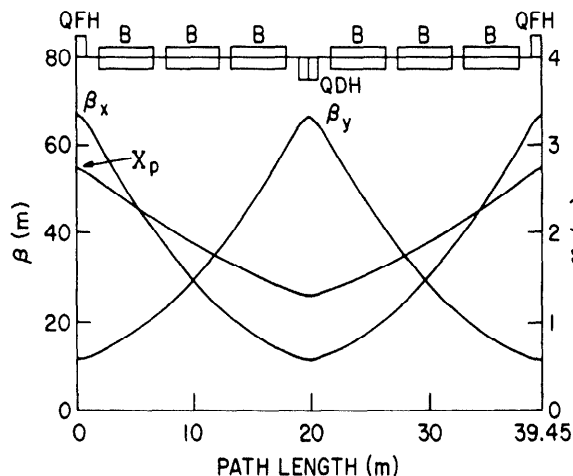
This could be achieved by separating the controls of the quadrupoles involved from that of the others and by choosing their gradients properly. Betatron and momentum matching across them would then be automatic (as it is now for the betatron motion alone) and the conditions in the crossing points could still be chosen freely. The advantages of this solution, which is presently under study, have to be weighed against the hardware consequences it involves.

Orbit Corrections

The various errors in the magnetic fields cause errors in the closed orbits, vertical dispersion in the crossing points, distortion of the working line, coupling between the horizontal and vertical components of the betatron motion, linear and non-linear stopbands and random variations in the β_x^* and β_y^* in the crossing points. These effects have been studied and correction coils have been provided when considered necessary.[1]

ISA Parameters

Table II presents the main parameters of the ISA lattice as presently planned.

Table II

Injection energy (γ inj)	31.4
Maximum energy (γ at 400 GeV)	426.3
Magnetic field in dipoles (γ inj)	0.368 T
Magnetic field in dipoles (400 GeV)	5.004 T
Gradient in cell quadrupoles (400 GeV)	60.1 T/m
Circumference ($= 4.75 \times C_{AGS}$)	3833.8 m
Periodicity	6
Regular cells (no x length)	6 x 9 x 39.5 m
Insertions (no x length + length)	6 x (141.722 + 141.775) m
Horizontal beam separation in arcs	0.95 m
Regular cell length (inner arc)	39.44 m
Regular cell length (outer arc)	39.55 m
Average radius of curvature in arcs	339.4 m
Radius of curvature in dipoles	266.6 m
Average radius of rings	610.2 m
Crossing angle	11.188 mrad
Betatron tunes ($\nu_H \approx \nu_V$)	22.62
Tune spread on working line ($\Delta\nu_H = \Delta\nu_V$)	~ 0.02
Transition energy (γ_{tr})	18.68
Phase slip factor at injection (γ)	1.85×10^{-3}
Horizontal amplitude functions in cell (β_{Hmax}, β_{Hmin})	67, 11.5 m
Vertical amplitude functions in cell (β_{Vmax}, β_{Vmin})	67, 11.5 m
Dispersion function in cell (X_{pmax}, X_{pmin})	2.73, 1.31 m
Phase advances per cell ($\Delta\psi_H/2\pi$, $\Delta\psi_V/2\pi$)	0.2515, 0.2515
Amplitude functions in crossing point (β_H^*, β_V^* in standard insertion)	40, 7.5 m
Dispersion in crossing point (X_p^*)	0
Maximum value of amplitude functions ($\hat{\beta}_H$, $\hat{\beta}_V$)	195.8, 154.9 m
Phase advances across insertions ($\Delta\psi_H/2\pi$, $\Delta\psi_V/2\pi$)	1.5, 1.5
Uncorrected linear chromaticity	-33
Operating chromaticity ($X_H - X_V$)	+2

Acknowledgment

References

1. G. Parzen, Report to this Conference.

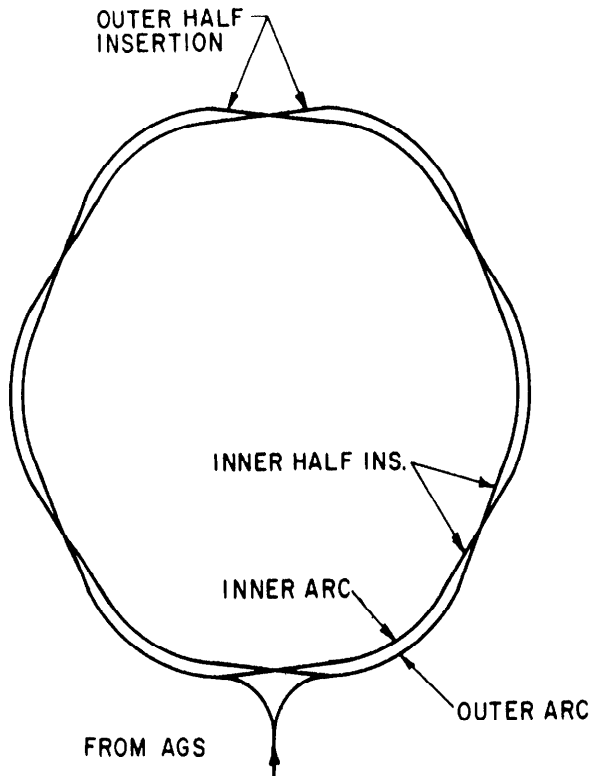Fig. 4. Betatron functions in standard cell.

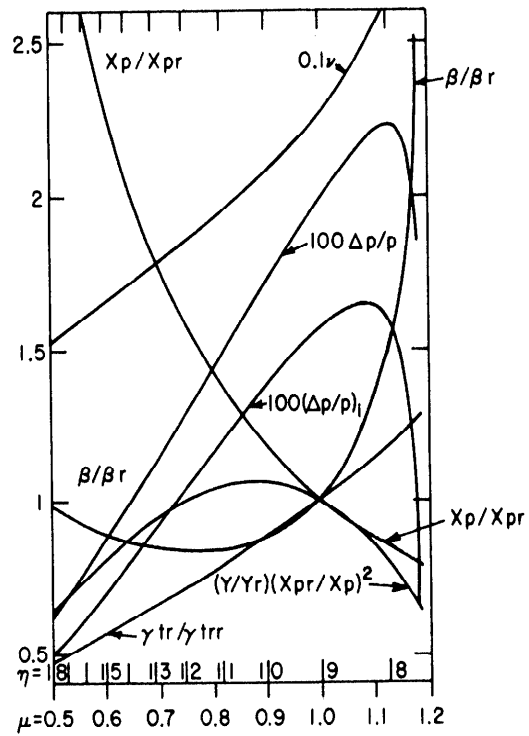Fig. 1. Topology of ISABELLE

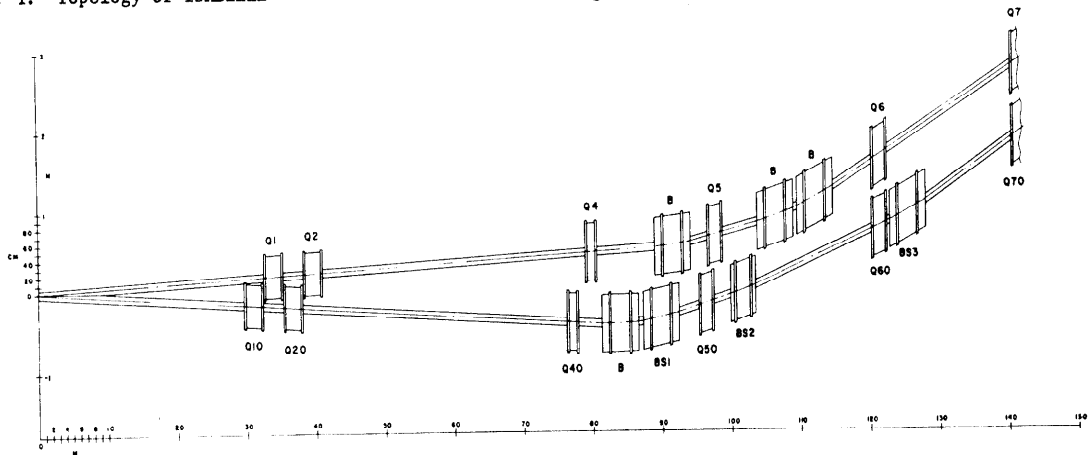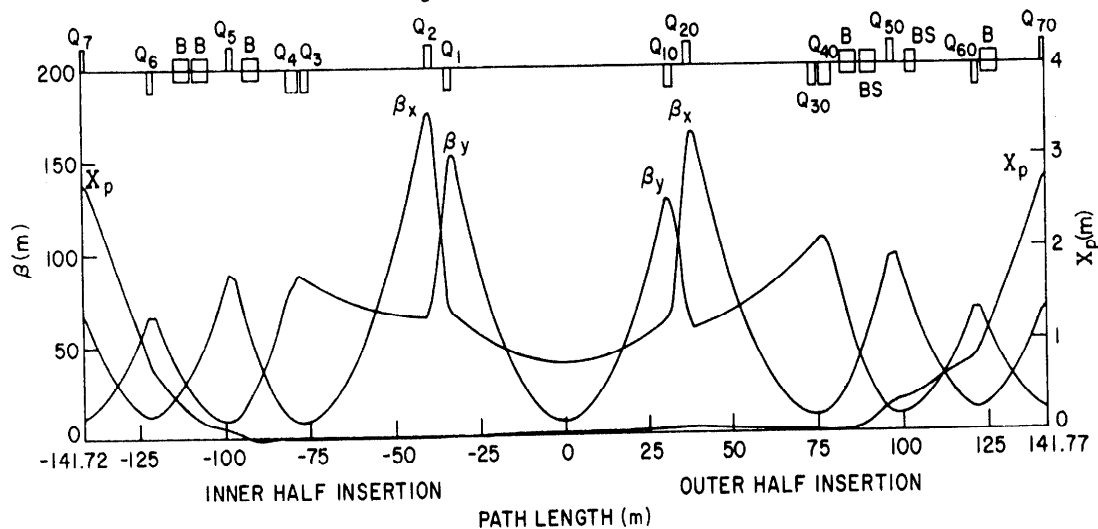Fig. 2. Betatron functions and acceptances.

Fig. 3. Insertion Geometry.

Fig. 5. Betatron functions in insertion.

3555